

# Locational Dependence of PV Hosting Capacity Correlated with Feeder Load

Kyle Coogan, Matthew J. Reno, and Santiago Grijalva  
School of Electrical and Computer Engineering  
Georgia Institute of Technology  
Atlanta, Georgia USA

Robert J. Broderick  
Photovoltaics and Distributed Grid Integration  
Sandia National Laboratories  
Albuquerque, NM, USA

**Abstract** — With rising adoption of solar energy, it is increasingly important for utilities to easily assess potential interconnections of photovoltaic (PV) systems. In this analysis, we show the maximum feeder voltage due to various PV interconnections and provide visualizations of the PV impact to the distribution system. We investigate the locational dependence of PV hosting capacity by examining the impact of PV system size on these voltages with regard to PV distance and resistance to the substation. We look at the effect of increasing system size on line loading and feeder violations. The magnitude of feeder load is also considered as an independent variable with repeated analyses to determine the effect on the PV impact analysis. A technique is presented to determine and visualize the maximum capacity for possible PV installations for distribution feeders.

**Index Terms** — distributed power generation, photovoltaic systems, power distribution, power system interconnection, power system modeling, solar power generation

## I. INTRODUCTION

As adoption of distributed generation continues to rise, an increasing amount of solar, among other renewables and generation sources, are being interconnected directly to the distribution grid [1]. With increasing photovoltaic (PV) generation on distribution feeders comes various benefits. PV systems, and other DG, have been shown to improve distribution system losses and voltage profiles [1], [2]. It can also lead to increased reliability as well as the deferment of transmission and distribution infrastructure and capacity upgrades [1].

In order to most fully and effectively realize these potential benefits, it is necessary to understand the associated concerns of increased interconnection of PV systems on the distribution system. Two common concerns of the interconnection of these systems are steady-state over-voltage and line-loading violations [3]. Therefore, before interconnections are approved by utilities, they must go through an interconnection impact study to thoroughly investigate the potential adverse effects of a project [4].

Currently, such screening processes can be time consuming and expensive, a problem that is only worsened by increasing penetration levels. With increasing numbers of these installations, it is becoming increasingly important for utilities to quickly assess potential interconnections of PV.

When conducting the analysis, several aspects of the feeder should be considered including losses, feeder capacity, voltage regulation equipment, and protection [5]. Initially, fixed power factor PV systems producing only real power will be considered as they are most common [6], but future work will consider PV with active voltage control [7]. EPRI has performed significant research in the area of feeder hosting capacity for PV [8], [9]. While their research was focused on determining the hosting capacity for the entire feeder, our research builds on this to investigate individual areas of the feeder to determine the local maximum.

In this analysis, we show the impact on maximum feeder voltage due to connecting a range of PV sizes on various buses. We also show the effect of these installations on line loading and feeder violations. These impacts are then examined under different magnitudes of feeder load. We then examine these same buses to determine the maximum central PV installation possible under various magnitudes of feeder load before resulting in a thermal or voltage violation on the feeder.

## II. METHODOLOGY

The circuit used for this initial analysis is EPRI test circuit 7 (Ckt7) available online at [10]. The topology of this feeder can be seen in Figure 1. The feeder is a short (4 km), 12.47 kV feeder with mostly industrial customers. This feeder has 288 buses on the medium-voltage 12.47 kV system, 200 of which are three-phase. For voltage regulation, Ckt7 has two switching capacitors but no load tap changer (LTC) at the substation or voltage regulators in the feeder. The substation transformer includes 14 feeders and is connected to a strong, 115 kV transmission system. The full-load demand at the substation is 36,111 kVA at 0.95 lagging power factor. The feeder loads use a conservation voltage reduction (CVR) load model that changes the power slightly based on the voltage, using values of 0.8 for real and 3.0 for reactive power [11].

To examine the impact of central PV installations on the feeder, an extensive process is used to step through all considered locations, storing data from the power flow solution for each scenario. The set of scenarios include a significant range of system sizes and locations. Due to the fact that Ckt 7 is an industrial feeder, the focus of the analysis is on single, large-scale, central PV plants. The PV systems were sized ranging from 0 to 10 MW in 100 kW increments,

---

This research was funded by Sandia National Laboratories, prepared under Contract No. 903634. Sandia National Laboratories is a multi-program laboratory managed and operated by Sandia Corporation, a wholly owned subsidiary of Lockheed Martin Corporation, for the U.S. Department of Energy's National Nuclear Security Administration under contract DE-AC04-94AL85000.

and all three-phase buses were considered. For each of the 100 considered system sizes at each of the 200 three-phase buses, a total of 20,000 snapshot power flow simulations were performed. Each power flow simulation is performed in full detail for the distribution feeder with hundreds of components, complex voltage regulation controls, and feeder loads allocated on the secondary system at the end of triplex lines. The unbalanced three-phase power flow is solved using the distribution system software OpenDSS [12] with GridPV [13] to perform analysis in MATLAB. During each power flow simulation, the maximum per unit bus voltage on the feeder is recorded, along with the maximum line loading (line current/line rating) of all lines. The solutions from the power flow simulations for each PV study case are analyzed to determine any violations or limitations in the distribution system that would not allow the particular interconnection.

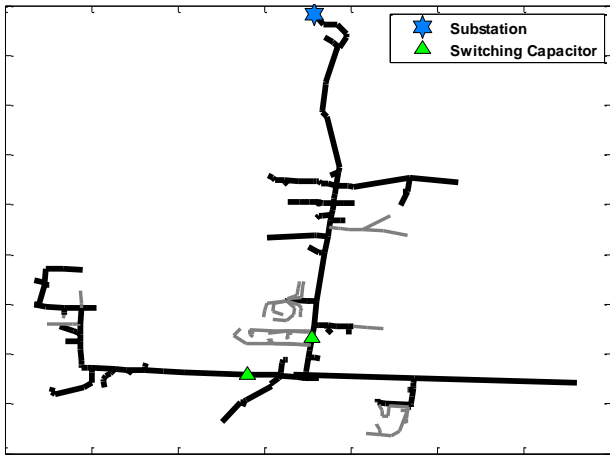


Figure 1. Ckt7 Topology and Voltage Regulation – black lines indicate three-phase.

The same three-phase buses were iterated through to determine the maximum allowed PV system size before resulting in an over-voltage violation or a line over-loading anywhere on the feeder. Voltage violations are classified as anything outside of Range A of ANSI C84.1 [14], and the line over-loading threshold is set at 100% of the normal line rating. Each bus was considered individually to find the maximum possible PV size, with a 50 kW resolution, before a violation occurs. Figure 2 shows a flow chart of the methodology employed for this analysis.

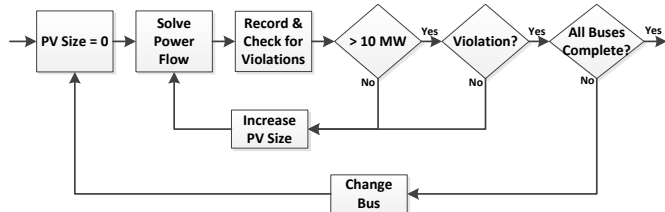


Figure 2. Flow chart of methodology.

For each scenario, the worst case is simulated with the PV system outputting rated power at unity power factor. Various magnitudes of feeder load were considered. It was found that over the year, the minimum daytime (9 am to 3 pm) load is

approximately 40% of the feeder peak load, and the average daytime load is 61% of the feeder peak. The daytime load is less than 50% of the feeder peak only 17% of the time, so the minimum load considered is 50%. The maximum load considered is 100%. Together these two scenarios respectively represent the worst and best case scenarios for connecting a system with rated output to the feeder.

### III. RESULTS

Maximum bus voltage was the first attribute examined in the analysis. Figure 3 shows the distribution of the maximum bus voltage due to installing a central PV system at various locations for the 50% load case as PV system size increases from 0 to 10 MW.

To reiterate the methodology and how this graph was obtained, there are data for every 0.1 MW step along the x-axis for system sizes ranging from 0.1 MW to 10 MW. For each of these PV system sizes, there are 200 scenarios with power flow solutions, corresponding to each of the three-phase buses, which consider each of the possible interconnection locations. For each of these scenarios, the maximum bus voltage on the feeder (in pu) was found. The combination of these 200 points for each of these 101 system sizes (including base case 0 MW) yields the distribution shown. For example, consider the case of a 10 MW PV system. For this system size, approximately 25% of the 200 potential three-phase buses will result in a max bus voltage above 1.05 pu. Therefore, for a 10 MW central PV system on Ckt 7, there are 150 buses at which this plant can be connected that will not result in an over-voltage violation given 50% load and rated PV output.

It is important to note that Figure 3 is the maximum voltage anywhere in the feeder. There is a clear point around 1.3 MW below which any interconnection of central PV will not cause a PCC voltage to be larger than the substation; therefore, the highest voltage occurs near the substation. As the PV size increases above this point, more interconnection locations will have PCC bus voltages that are larger than the substation, depending on their distance from the substation. Buses furthest from the substation will deviate first. These further buses will have PCC bus voltages that increase at a faster rate with increases in system size, as illustrated by the increasing spread among the percentiles.

The median maximum bus voltage does not surpass 1.05 pu at 10MW. However, line thermal limits make any analysis of larger systems impractical.

The plot from Figure 3 was replicated for maximum line loading and is shown in Figure 4. The maximum line loading for each of the 200 interconnection locations was determined considering each of PV system sizes.

The impact on line loading is significantly more clustered than the impact on bus voltage. For example, when considering a 3.5 MW system, none of the scenarios result in over-loading. However, when considering a 3.9 MW system, over 50% of the scenarios result in over-loading. This is due to distinct cable types used throughout a feeder. A given distribution system generally only has a few different cable sizes. In this case, all three-phase laterals have the same line rating and overload at the same time.

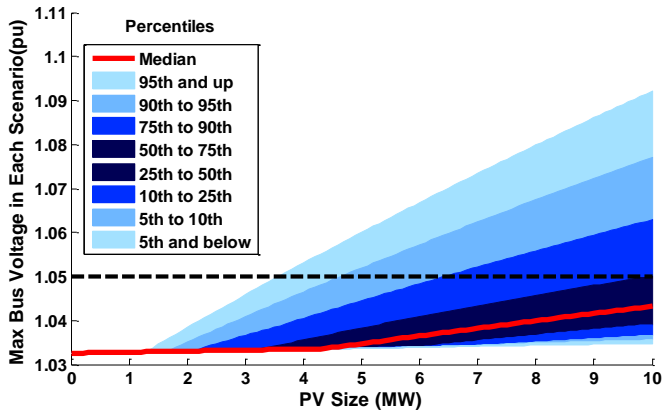


Figure 3. Effect of PV size on max bus voltage under 50% load.

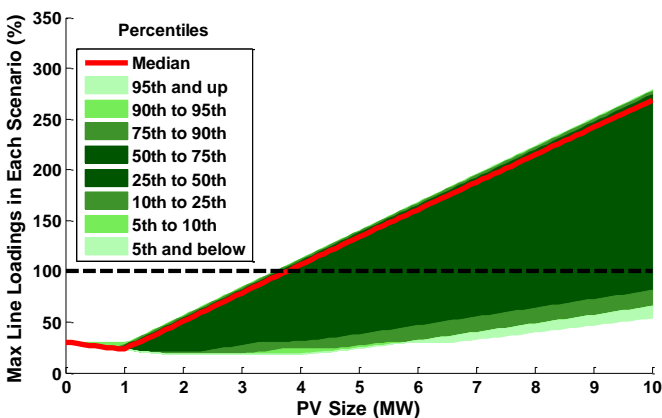


Figure 4. Effect of PV size on max line loading under 50% load.

The same data used for Figure 3 was analyzed using the distance of the PV interconnection to the substation as an independent variable. Each data point in Figure 5 represents a power flow solution with the maximum bus voltage plotted as a function of this distance and colored to indicate the PV system size. Figure 5 validates the difference in slopes between percentile ranges in Figure 3. Interconnections toward the end of the feeder exhibit a wider range of maximum voltages, and therefore a larger response to differences in system size.

The feeder backbone is clearly noticeable towards the bottom of Figure 5. On the backbone particularly close to the substation, increases in system size have a relatively small effect on the PCC bus voltage. System size exhibits less impact on these buses than it does on other buses with higher impedances between the PCC and the substation. For these buses on the backbone and close to the substation (less than 0.5 km), the highest bus voltage will be that of the substation. The increase in maximum voltage for these cases is not due to the PCC bus voltage, but rather an increase in substation voltage due to the marginal decrease in load being served by the substation.

However, when the PV is further away from the substation on the feeder backbone, the increased resistance

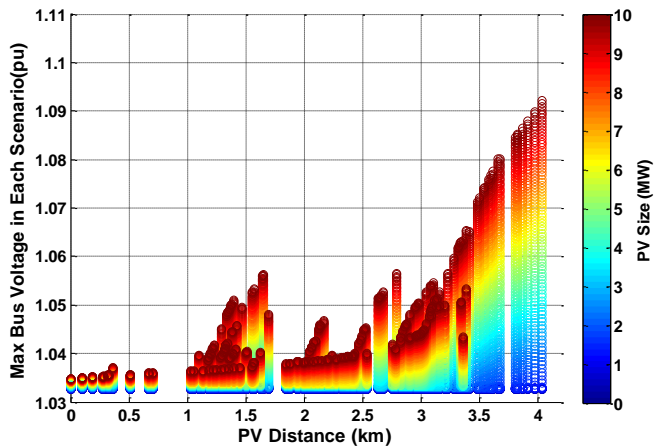


Figure 5. PV size and distance effect on max bus voltage under 50% load.

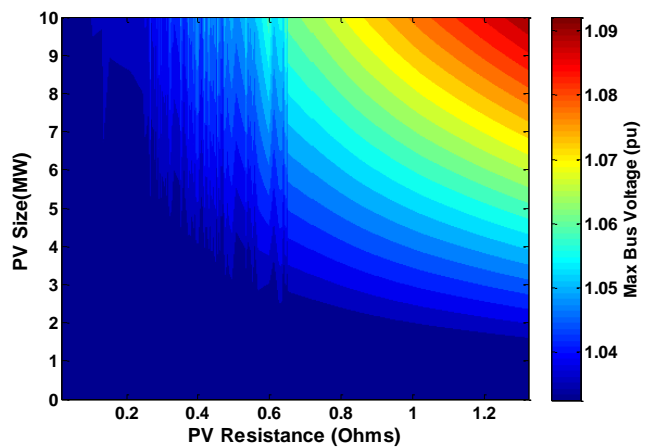


Figure 6. Max bus voltage as a function of PV size and resistance under 50% load.

causes the impact of system size on PCC bus voltage to increase. This results in the linear trend at the bottom of the graph from 1 km to 2.5 km shown by the dark red points indicating a 10 MW system size, which indicates a larger maximum bus voltage for the same system size. There is also some deviation from this linear trend. This is due to the higher impedance laterals that separate from the backbone relatively close to the substation. These higher impedance laterals have a distance to the substation equivalent to other locations that are downstream on the backbone, but their increased resistance causes the system size to have a greater impact on their PCC bus voltage.

Given this impact of PCC impedance to the substation, the same data was then analyzed using this impedance as well as PV system size as the independent variables. We examined the impact of these variables on the maximum feeder bus voltage, which is shown by the contour in Figure 6.

As expected, this creates a smooth relationship for most of the region. However, differences in the load sizes downstream from the PCC bus causes the irregularities observed up to around 0.7  $\Omega$ . A PCC bus with larger downstream load will, in the base case, have a lower voltage than another PCC bus with the same impedance but less downstream load.

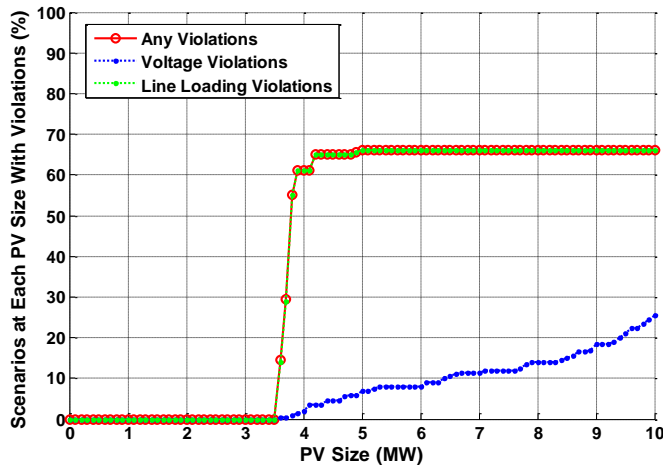


Figure 7. Percent of PV scenarios at each PV size with violations under 50% load.

As PV system size is increased, the impact of the system size on each PCC voltage will be the same, with the voltages differentiating by this initial discrepancy. A PCC bus with larger downstream load will always have a lower PCC bus voltage for a given system size than will a bus with larger downstream load. Therefore, the maximum bus voltage will be the substation voltage more often for cases with large amounts of downstream load. This is illustrated later in Figure 11 by considering the maximum bus voltage for various feeder loads.

After analyzing the effect of PV system size on bus voltage and line loading separately it is useful to observe the effect in terms of overall violations. Figure 7 shows the percentage of locations for a given PV size that result in any violation, either over-voltage or line-loading, as we increase PV system size for the 50% load case. The results are also shown for only considering over-voltage violations and only considering line-loading violations.

Around 3.6 MW there is a drastic increase in any violations from zero violations to over 50% of the considered scenarios at 3.9 MW. This is due to how similarly the line loading profiles increase together and was mentioned in the discussion of Figure 4.

After observing the effect of PV system size on scenario violations, we looked at the maximum system size allowed at each of the 200 PCC buses before a violation occurred for both the half-load and the peak-load cases. The maximum possible PV system sizes are plotted on the circuit topology, shown in Figure 8 and Figure 9, varying both marker size and color to correspond to relative maximum system size.

This clearly shows the PCC locations that are causing the line-loading violations and the large disparity between allowed system sizes on the backbone versus that of the laterals. However, these figures also show an interesting similarity: there is little difference when considering the half-load and the peak-load case between the maximum allowed PV system size on a bus. When the load is doubled the maximum PV system size allowed on the feeder increases 8.4% from 14.95 MW to 16.2 MW. The average increases 4.6% from 6.55 MW to 6.86 MW. Because the limit for maximum PV system size allowed is generally a result of the line ratings on this feeder, the change in allowed PV size

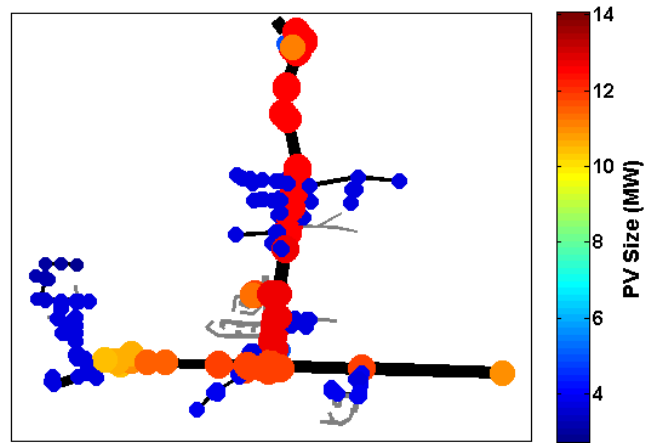


Figure 8. Maximum allowed PV size at a single bus under 50% load.

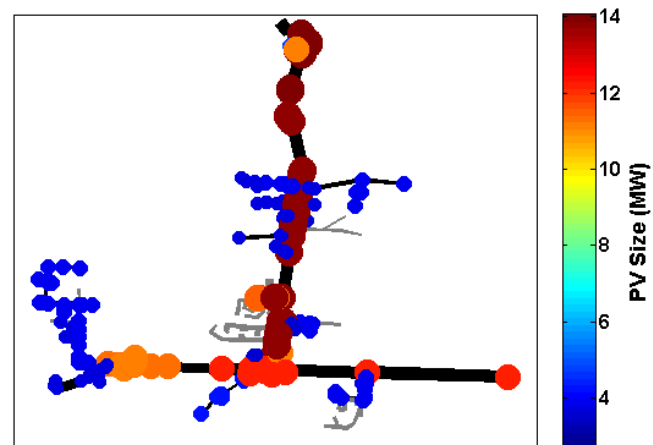


Figure 9. Maximum allowed PV size at a single bus under peak load.

under different values of feeder load is a function of the downstream load. For example, the change in current flow through a lateral is similar for different load magnitudes, so the maximum allowed PV system size has little change.

The effects of increasing PV system size on line loading was observed for both the 50% load and 100% load case together and is shown in Figure 10. These curves were obtained by taking the maximum of the line loadings for each of the 200 PCC scenarios at each PV system size. Essentially, each line is the top edge of the graph shown in Figure 4 for a given line loading. This allows a concise visualization of the effects of feeder load on maximum line loading.

The effect of the difference in feeder load is clearly evident with the base case comparison (i.e. observing the line loadings when the system size equals 0 MW). The change in load also affects the point at which the line connected to the PCC becomes the most heavily loaded line, as shown by the elbows in the curve. However, once the line connected to the PCC becomes the most heavily loaded line, the curves remain almost identical as PV system size increases.

Under the conditions of high levels of PV at 10 MW, it may not be initially intuitive that the case with 100% of peak feeder load has a higher line loading percent, but this is a result of the PCC voltage. Since the larger peak load causes the PCC voltage to be slightly lower, the current output of the PV plant is slightly higher to maintain the same power output.

A similar plot for maximum bus voltage is shown in Figure 11, which considers the 60% and 90% load cases as well. As before, this plot is essentially the top edge of the graph shown in Figure 3. Similar to Figure 10, the base case comparison when the system size equals 0 MW clearly shows the difference in loads by showing the differing substation voltages, which are the maximum feeder voltages in each case for the base case with no PV generation. This higher initial voltage for the entire feeder causes a vertical shift throughout the range of scenarios. The difference in load also changes the point at which the PCC bus voltage becomes the highest in the system.

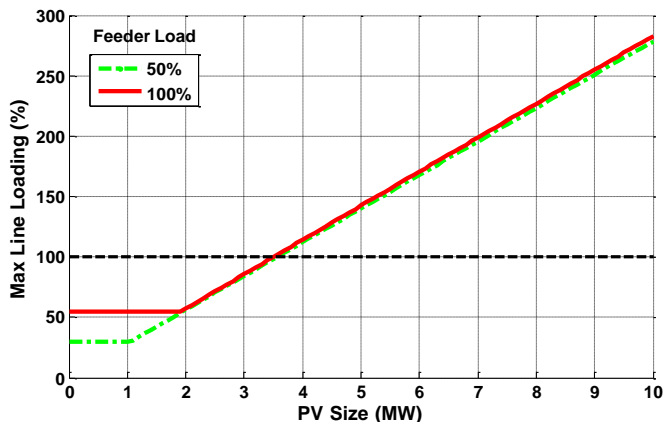


Figure 10. Maximum line loading for all PV scenarios at each PV size.

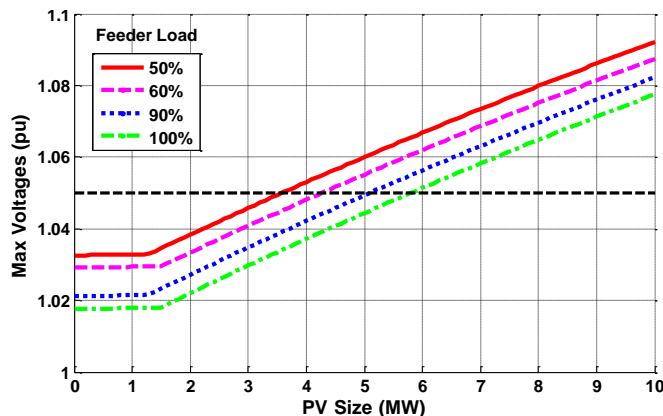


Figure 11. Maximum bus voltage for all PV scenarios at each PV size.

#### IV. FUTURE WORK

For this industrial feeder, large-scale, individual PV plants were considered, but the analysis methodology can also be used for high penetrations of distributed residential rooftop PV systems. We aim to expand steady-state analysis to include more PV plant parameters such as changing power factor [15] and a wider array of feeder parameters such as short-circuit current and downstream load. One main concern of high penetration of PV systems is their variability, particularly with penetrations above 20% [5], [6]. We will also expand these methods by performing time-series analyses of central and distributed PV to study the impact of solar variability on voltage regulator operations [16]. Finally, we will apply these methods to a larger range of feeders to develop a generalized technique of modeling the likelihood of

different effects an interconnection may have based on the feeder type, feeder characteristics, PV location, PV plant size and configuration, and deployment level. This will eventually result in a risk being associated with different PV interconnections.

#### V. CONCLUSIONS

The impacts of a central PV system on various locations of a feeder were analyzed for multiple PV system sizes and feeder loads. It was found that for the example feeder Ckt7, the size of the PV plant, regardless of location, is mostly impacted by thermal limits as opposed to voltage limits. For this feeder, the feeder load has little impact on the allowed system size before these thermal violations occur. With regard to voltage violations, the biggest factor is impedance from the PCC to the substation. The location of PV on the feeder, because of its impact on impedance to the substation, will affect the rate at which an increase in PV size increases PCC voltage. Ultimately, these methods will serve as a basis for continuing to formulate a technique for identifying key criteria and circuit parameters to establish the likelihood of feeder impact due to high penetrations of PV.

#### VI. REFERENCES

- [1] P. P. Barker and R. W. De Mello, "Determining the impact of distributed generation on power systems. I. Radial distribution systems," in *IEEE Power Engineering Society Summer Meeting*, 2000.
- [2] E. K. Bawan, "Distributed generation impact on power system case study: Losses and voltage profile," in *22nd Australasian Universities Power Engineering Conference (AUPEC)*, 2012, pp. 1-6.
- [3] A. Hoke, R. Butler, J. Hambrick, and B. Kroposki, "Steady-State Analysis of Maximum Photovoltaic Penetration Levels on Typical Distribution Feeders," *IEEE Transactions on Sustainable Energy*, 2012.
- [4] R. J. Broderick, J. E. Quiroz, M. J. Reno, A. Ellis, J. Smith, and R. Dugan, "Time Series Power Flow Analysis for Distribution Connected PV Generation," Sandia National Laboratories SAND2013-0537, 2013.
- [5] D. T. Rizy, L. Fangxing, L. Huijuan, S. Adhikari, and J. D. Kueck, "Properly understanding the impacts of distributed resources on distribution systems," in *IEEE PES General Meeting*, 2010, pp. 1-5.
- [6] G. J. Shirek and B. A. Lassiter, "Solar plant modeling impacts on distribution systems PV case study," in *IEEE Rural Electric Power Conference (REPC)*, 2012.
- [7] M. J. Reno, R. J. Broderick, and S. Grijalva, "Smart Inverter Capabilities for Mitigating Over-Voltage on Distribution Systems with High Penetrations of PV," in *IEEE Photovoltaic Specialists Conference*, Tampa, FL, 2013.
- [8] J. W. Smith, R. Dugan, M. Rylander, and T. Key, "Advanced distribution planning tools for high penetration PV deployment," in *Power and Energy Society General Meeting, 2012 IEEE*, 2012, pp. 1-7.
- [9] "Stochastic Analysis to Determine Feeder Hosting Capacity for Distributed Solar PV," EPRI, Technical Report 1026640, 2012.
- [10] EPRI. (8/2013). *EPRI Test Circuits*. Available: <http://ewh.ieee.org/soc/pes/dsacom/testfeeders/>
- [11] "Distribution Green Circuits Collaboration," EPRI, Technical Report 1020740, 2010.
- [12] EPRI. (2013). *Open Distribution System Simulator*. Available: <http://sourceforge.net/projects/electricdss/>
- [13] M. J. Reno and K. Coogan, "Grid Integrated Distributed PV (GridPV)," Sandia National Laboratories SAND2013-6733, 2013.
- [14] ANSI Standard C84.1-2011 American National Standard For Electric Power Systems and Equipment - Voltage Ratings (60 Hz).
- [15] M. J. Hossain, T. K. Saha, and N. Mithulananthan, "Impacts of wind and solar integrations on the dynamic operations of distribution systems," in *Australasian Universities Power Eng. Conference*, 2011.
- [16] J. E. Quiroz, M. J. Reno, and R. J. Broderick, "Time Series Simulation of Voltage Regulation Device Control Modes," in *IEEE Photovoltaic Specialists Conference*, Tampa, FL, 2013.